J Appl Biotechnol Rep. 2025 September;12(3):1701-1711

Journal of
Applied Biotechnology Reports

doi 10.30491/jabr.2025.498830.1827

Original Article

In Silico Screening of Theophylline Derivatives for Anticancer Activity: Integrating Molecular Docking, ADMET Predictions, and Molecular Dynamics Simulations

Fatima Zohra Fadel [1,2*], Noureddine Tchouar [1], Khadidja Smail [1,2], Wafaa Cheikh [1], Mohammed Arab Ait Tayeb [1], Sofiane Benmetir [1,3], Karim Ouadah [1], Fatima Soualmia [1], Sihem Medjahed [1]

[1] Laboratory of Environmental Process Engineering (LIPE), Faculty of Chemistry, University of Science and Technology of Oran Mohamed Boudiaf (USTO-MB), BP 1505, El Mnaouer, Bir El Djir 31000, Oran, Algeria
[2] Department of Biotechnology, Faculty of Natural and Life Sciences, University of Science and Technology of Oran Mohamed Boudiaf (USTO-MB), BP 1505, El Mnaouer, Bir El Djir 31000, Oran, Algeria
[3] Department of Physical Chemistry, Faculty of Pharmacy, University of Valencia, Av. Vicent Andrés Estellés s/n, 46100 Valencia, Spain

Corresponding Author: Fatima Zohra Fadel, PhD Candidate, Laboratory of Environmental Process Engineering (LIPE), Faculty of Chemistry, University of Science and Technology of Oran Mohamed Boudiaf (USTO-MB), BP 1505, El Mnaouer, Bir El Djir 31000, Oran, Algeria. Tel: +213660682309, E-mail: fatimazohra.fadel@univ-usto.dz

Received January 9, 2025; **Accepted** May 3, 2025; **Online Published** September 30, 2025

Abstract

Introduction: Aldehyde dehydrogenase 1A1 (ALDH1A1) is an enzyme involved in cellular detoxification and plays an important role in maintaining cancer stem cells and chemoresistance. This study explores the potential of four theophylline derivatives (compounds A, B, C, and D) as ALDH1A1 inhibitors using molecular docking, ADME analysis, toxicity predictions, and molecular dynamics simulations.

Materials and Methods: Four compounds were chosen based on their strong experimental and predicted biological activities. Docking with human ALDH1A1 was performed using AutoDock Vina (v1.1.2), while ADMET properties were assessed with ADMETlab 3.0 and ProTox 3.0. Molecular dynamics simulations were carried out with GROMACS 2024.2 to evaluate the dynamic behavior and binding stability of the complexes.

Results: Molecule A showed the highest binding affinity (–11.3 kcal/mol) and established substantial interactions with important residues such as TRP178, TYR297, and PHE171. ADMET analysis indicated that compounds A and C have high intestinal permeability, and all compounds displayed low toxicity risks, supporting their promise as therapeutic candidates. Molecular dynamics simulations confirmed that ALDH1A1's overall structure remains stable during the simulation and revealed strong hydrogen bonding in complex A, as supported by favorable RMSD, SASA, and RMSF values.

Conclusions: The integrated approach combining molecular docking, ADMET analysis, and molecular dynamics simulations confirms that Molecule A is the most promising ALDH1A1 inhibitor, exhibiting stable binding, favourable pharmacokinetic properties, and robust interactions with several residues. These results provide a strong foundation for further experimental validation and optimization in the development of targeted cancer therapies.

Keywords: Theophylline Derivatives, ALDH1A1 Inhibitors, Cancer, Molecular Docking, ADMET, Molecular Dynamics

Citation: Fadel FZ, Tchouar N, Smail K, Cheikh W, Ait Tayeb MA, Benmetir S, et al. *In Silico* Screening of Theophylline Derivatives for Anticancer Activity: Integrating Molecular Docking, ADMET Predictions, and Molecular Dynamics Simulations. J Appl Biotechnol Rep. 2025;12(3):1701-1711. doi:10.30491/jabr.2025.498830.1827

Introduction

Aldehyde dehydrogenase 1 family member A1 (ALDH1A1) plays a key role in detoxifying reactive aldehydes, thereby reducing oxidative stress and protecting cells from cytotoxic damage. It is particularly overexpressed in cancer stem cells (CSCs), contributing to chemoresistance, cell survival, and self-renewal.[1,2] ALDH1A1 is considered a promising target for cancer therapy, as its inhibition can reduce CSC viability and enhance sensitivity to chemotherapy, potentially preventing cancer relapse.[3,4]

Theophylline, a compound widely used as a bronchodilator, has demonstrated potential as an ALDH1A1 inhibitor, along with its anti-inflammatory, antimicrobial, and anticancer properties.[5,6] Its derivatives, especially those modified at the 7- and 8-positions, have shown therapeutic potential in cancer treatment, bronchospasm, and antimicrobial infections.[7] Additionally, recent studies suggest that combining theophylline with chemotherapeutic agents could enhance cancer treatment efficacy, especially for lung cancer.[8]

Building on these findings, this study introduces a novel approach for identifying potent theophylline derivatives as ALDH1A1 inhibitors. Four compounds (A, B, C, and D) were selected for molecular docking studies based on their high experimental and predicted biological activity. These compounds were downloaded from the PubChem database

after a comprehensive analysis of a larger set of candidates, ensuring that the selected molecules are the most promising for further investigation.

The primary objective of this research is to identify and characterize theophylline derivatives as inhibitors of ALDH1A1 through molecular docking simulations and ADMET profiling. Furthermore, a molecular dynamics study was performed to assess the binding stability and dynamic behavior of the ligand protein complexes. The molecular docking studies will focus on understanding the binding interactions between these compounds and the ALDH1A1 active site, predicting binding affinities, and identifying significant residues involved in binding. This will help elucidate potential mechanisms of inhibition. In addition, the pharmacokinetic properties and toxicity profiles of these compounds will be assessed through ADMET profiling, ensuring that only those with optimal safety and efficacy profiles are selected for further drug development.

By advancing this research, we aim to provide a targeted approach to cancers that overexpress ALDH1A1. This work could lead to the development of more effective and tailored cancer therapies with the potential for significant clinical impact.

Materials and Methods

Molecular Docking

Three-dimensional (3D) structures of theophylline derivatives (Table 1) were downloaded from PubChem and optimized using the B3LYP/6-31+(d,p) method in Gaussian 16 software package.[9] Conformations characterized by the lack of imaginary frequencies at energy minima were selected for docking. As a post-optimization step, Gasteiger charges were assigned, nonpolar hydrogens removed, and rotatable bonds defined for each ligand. This preparation enhanced flexibility during docking, ensuring an accurate depiction of ligand behaviour in the binding site.[10]

Table 1. 2D Structures and Experimental/Predicted pIC50 Values in µm of Selected Theophylline Derivatives for ALDH1A1 Inhibition

Compound	PubChem ID	Structure 2D	pIC 50 Exp (µm)	pIC 50 Pred (µm)
A	121365869	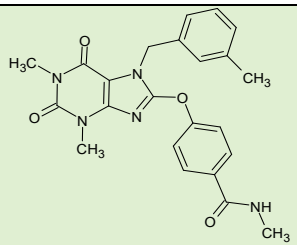	7.244	7.211
B	121370241	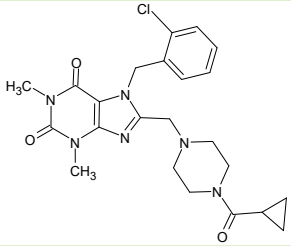	7.161	7.150
C	121370430	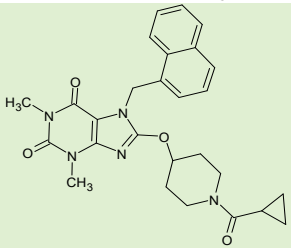	7.040	7.027
D	121365894	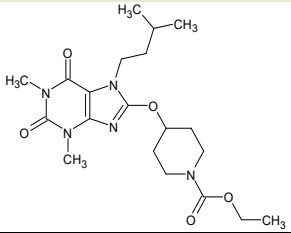	6.860	6.870

pIC 50 Predictive[11]

Docking of four ligands with human ALDH1A1 was performed using AutoDock Vina (v1.1.2) and AutoGrid in AutoDock Tools (ADT 1.5.7).[12] The ALDH1A1 structure (PDB ID: 7UM9, 1.8 Å) was retrieved, prepared by removing ligands, water, and heteroatoms, and optimized by

adding polar hydrogens and Kollman charges.[12] A grid box centered at X = 34.22, Y = -15.89, Z = 15.80 was created at the active site. Docking used the Lamarckian Genetic Algorithm (LGA).[13] Complexes were analysed in Discovery Studio (v2021)[14] for hydrogen bonding, hydrophobic interactions, and steric hindrances. Validation involved re-docking the co-crystallized inhibitor and calculating RMSD.[15]

ADME

ADME Predection

ADME (Absorption, Distribution, Metabolism, Excretion) analysis was performed to evaluate the pharmacokinetics of selected theophylline derivatives based on their docking interactions with human ALDH1A1.[16]

ADMETlab 3.0 was used for in silico predictions of bioavailability, solubility, permeability, metabolic stability, and enzyme interactions. Molecular structures were converted to SDF format using Open Babel for compatibility.[17] These predictions complement the docking results, helping to assess the likelihood of the compounds reaching the target site and exhibiting the desired pharmacological effects.

Toxicity Analysis

Toxicity was predicted using the ProTox 3.0 web server,[18] which utilizes machine learning models to assess endpoints such as acute oral toxicity (LD50), toxicity class, and potential biological targets. PubChem identifiers of the theophylline derivatives were used to input molecular data into ProTox 3.0.[19] This analysis, combined with docking results, helped identify compounds that bind effectively to ALDH1A1 while maintaining a safe toxicity profile for further development.

Molecular Dynamics Simulations

The topology parameters for the ligands were generated using ACPYPE (v. 2023.10.27)[20] with the General Amber Force Field (GAFF). The protein was prepared using GROMACS (v. 2024.2),[21] and its topology parameters were generated with the Amber99sb force field.[22] Each complex was solvated in a cubic box employing the Simple Point Charge (SPC) water model, and the systems were neutralized by adding three Na^+ ions. Energy minimization was carried out using the steepest descent algorithm for 50,000 steps until the maximum force (Fmax) was reduced below 300 kJ/mol.[23] Subsequently, the systems were equilibrated in two phases: first under an NVT (canonical) ensemble at 300 K for 500 ps with temperature controlled by the V-rescale algorithm, followed by equilibration under an NPT (isothermal-isobaric) ensemble for 500 ps, during which temperature and pressure were maintained constant using the V-rescale and Parrinello-Rahman algorithms,[24] respectively. Finally, the molecular dynamics (MD) simulations were performed for 100 ns under the NPT ensemble. Post-simulation, the trajectories were analyzed using GROMACS tools (The root mean square deviation **(**RMSD), radius of gyration (RG), The root mean square fluctuation (RMSF), solvent-accessible surface area (SASA), and hydrogen bonds).

Results and Discussion

Molecular Docking

Validation of the Molecular Docking Protocol

To ensure the reliability of the docking protocol, a re-docking experiment was conducted using the co-crystallized ligand from PDB structure 7UM9. The ligand was reintroduced into its original binding site, demonstrating the docking algorithm's ability to replicate experimental binding conformations. This method validates the computational model for predicting novel compound interactions.

The docking accuracy was measured by the root-mean-square deviation (RMSD) between experimental and predicted conformations. A RMSD value of 0.467 Å confirmed high precision, significantly below the 2 Å threshold for reliable simulations. This result underscores the robustness of the docking protocol for accurate predictions.

The re-docking results are visually represented in Figure 1, which overlays the docked ligand (in red) with the co-crystallized ligand (in blue), showcasing a near-perfect structural alignment.

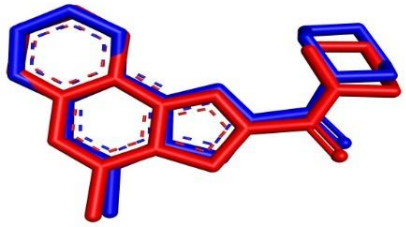

Figure 1. Re-docking pose with the RMSD value of 0.467 E (bleu = Original, red = Docked).

Furthermore, the binding energy of −9.8 kcal/mol further supports the protocol's validity, indicating stable and favourable interactions between the ligand and protein. Such strong binding affinities are critical for computational modeling in drug discovery.

Interactions of Theophylline Derivatives with ALDH1A1

The interactions of theophylline derivatives with ALDH1A1 were examined to understand their potential as enzyme inhibitors. Docking scores ranged from −11.3 to −9.4 kcal/mol (Table 2), with Compound A exhibiting the highest affinity (−11.3 kcal/mol). This strong binding is attributed to hydrogen bonds and hydrophobic interactions stabilizing the ligand-protein complex. Compounds B and C also showed significant affinities, while Compound D exhibited a weaker interaction.

Table 2. Docking Scores (kcal/mol) of Theophylline Derivatives within the Active Site of ALDH1A1

Compound	Affinity (kcal/mol)
A	-11.3
B	-10.6
C	-10.3
D	-9.4

Figure 2 illustrates the orientation of the theophylline derivatives within ALDH1A1's active site. Hydrogen bond (H-bond) positions vary between compounds (Figure 3), which may influence binding stability and ligand effectiveness. Each compound interacts through non-covalent forces like hydrogen bonding and hydrophobic interactions, key for their inhibitory potential.

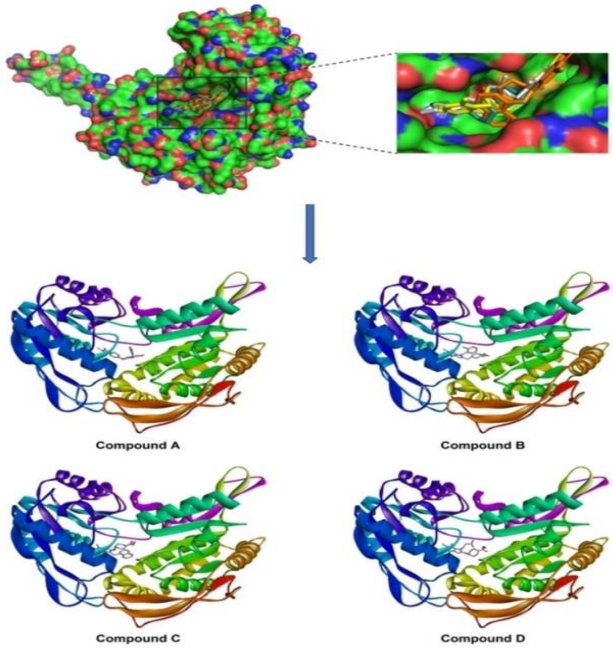

Figure 2. Orientation of the Four Theophylline Derivatives within the ALDH1A1 Active Site.

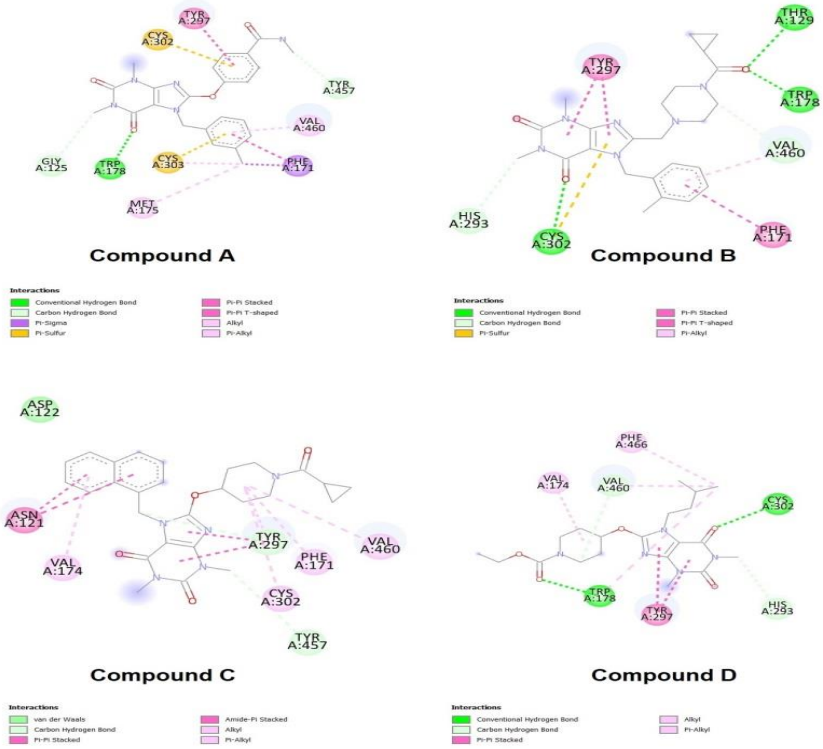

Figure 3. 2D Interaction Diagram of Theophylline Derivatives with ALDH1A1.

Table 3. Binding Interactions of Theophylline Derivatives with ALDH1A1 Protein

Compound	Active Amino Acid	Bond Length	Bond Type	Bond Category
A	TRP178	2,2569	Conventional H Bond	Hydrogen Bond
	GLY125	3,67482	Carbon Hydrogen Bond	Hydrogen Bond
	TYR457	3,50183	Carbon Hydrogen Bond	Hydrogen Bond
	PHE171	3,85084	Pi-Sigma	Hydrophobic
	CYS302	5,23625	Pi-Sulfur	Other
	CYS303	5,71165	Pi-Sulfur	Other
	TYR297	3,7348	Pi-Pi Stacked	Hydrophobic
	PHE171	4,94688	Pi-Pi T-shaped	Hydrophobic
	MET175	5,02514	Alkyl	Hydrophobic
	CYS303	4,54298	Alkyl	Hydrophobic
	VAL460	4,64886	Pi-Alkyl	Hydrophobic
B	THR129	2,71304	Conventional H Bond	Hydrogen Bond
	TRP178	2,10997	Conventional H Bond	Hydrogen Bond
	CYS302	3,64622	Conventional H Bond	Hydrogen Bond
	HIS293	3,64601	Carbon Hydrogen Bond	Hydrogen Bond
	VAL460	2,97206	Carbon Hydrogen Bond	Hydrogen Bond
	CYS302	5,97427	Pi-Sulfur	Other
	TYR297	3,95331	Pi-Pi Stacked	Hydrophobic
	TYR297	3,94995	Pi-Pi Stacked	Hydrophobic
	PHE171	4,78981	Pi-Pi T-shaped	Hydrophobic
	VAL460	4,72822	Pi-Alkyl	Hydrophobic
C	TYR457	3,47596	Carbon Hydrogen Bond	Hydrogen Bond
	TYR297	3,43691	Carbon Hydrogen Bond	Hydrogen Bond
	TYR297	5,2358	Pi-Pi Stacked	Hydrophobic
	TYR297	3,9979	Pi-Pi Stacked	Hydrophobic
	ASN121	5,4539	Amide-Pi Stacked	Hydrophobic
	ASN121	4,13288	Amide-Pi Stacked	Hydrophobic
	CYS302	5,36742	Alkyl	Hydrophobic
	VAL460	5,24653	Alkyl	Hydrophobic
	PHE171	5,41442	Pi-Alkyl	Hydrophobic
	TYR297	5,15271	Pi-Alkyl	Hydrophobic
	VAL174	5,21049	Pi-Alkyl	Hydrophobic
D	TRP178	2,0054	Conventional H Bond	Hydrogen Bond
	CYS302	3,69483	Conventional H Bond	Hydrogen Bond
	VAL460	3,49955	Carbon Hydrogen Bond	Hydrogen Bond
	HIS293	3,48815	Carbon Hydrogen Bond	Hydrogen Bond
	TYR297	3,70891	Pi-Pi Stacked	Hydrophobic
	TYR297	3,89838	Pi-Pi Stacked	Hydrophobic
	VAL174	5,37457	Alkyl	Hydrophobic
	VAL460	3,80821	Alkyl	Hydrophobic
	TRP178	4,81032	Pi-Alkyl	Hydrophobic
	PHE466	4,594	Pi-Alkyl	Hydrophobic

Differences in H-bond positioning suggest some derivatives bind more efficiently, affecting enzyme inhibition. Table 3 summarizes interactions with key residues, such as TRP178, TYR297, PHE171, VAL460, and CYS302, critical for stabilizing the ligand-enzyme complex. For instance, compound B forms strong H-bonds with TRP178 (2.10997 Å) and THR129 (2.71304 Å), while compound D exhibits a shorter H-bond with TRP178 (2.0054 Å), indicating higher binding energy.

Hydrophobic interactions are vital for stabilizing the ligand-receptor complex. Key residues like TYR297, PHE171, and VAL460 enhance ligand stability through π-π stacking, π-alkyl, and alkyl interactions. For example, compound A demonstrates π-π stacking with TYR297 (3.7348 Å) and π-sigma interactions with PHE171 (3.85084 Å). Compound C also exhibits strong π-π stacking with TYR297 (3.43691 Å), contributing to thermodynamic stability.[25]

These variations across PDB structures highlight different ligand-enzyme configurations. Additionally, MET175 interaction in compound A indicate selective binding, enhancing specificity and potential as an ALDH1A1 inhibitor.

In comparison, previous studies, including those by[25,26] focused on PDB structures 4X4L and 4WP7, respectively. These studies emphasized the importance of residues such as GLY125, THR129, and TRP178, which are central to electrostatic interactions within the enzyme's active site. Our results align with these findings, further supporting the critical roles of these residues in stabilizing the ligand-enzyme complex.

Building on these findings, among the tested derivatives, compound A stands out due to its interaction with MET175, a residue essential for ALDH1A1's catalytic functions, such as dehydrogenation and nitric oxide generation.[27] This interaction, alongside hydrophobic and electrostatic stabilization by TYR297 and VAL460, underscores its potential as a therapeutic candidate. These findings provide a foundation for further optimization in drug design.

This study validated the docking protocol and provided insights into the binding interactions of theophylline derivatives

with ALDH1A1. Compound A demonstrated the highest binding affinity and specificity, positioning it as a leading candidate for therapeutic applications. The detailed analysis of hydrogen bonding and hydrophobic interactions involving residues such as TRP178, TYR297, and MET175 underscores their critical role in stabilizing the ligand-enzyme complex.

The docking results were compared with the co-crystallized ligand in PDB 7UM9, the interactions identified are described in Table 4. The comparison indicates that analysis of residual interactions revealed several key bonds in the studied complexes. The Pi-Sulfur interaction involving CYS302 is observed in complexes A, B as well as in the native ligand, with similar distances. The VAL460 residue, involved in Pi-Alkyl and Alkyl bonds stabilizing the hydrophobic environment, is present in the native ligand and in complexes A, B, C and D, with distances varying between 2.97 and 5.24 Å. The Alkyl interaction of CYS303, identified in the native ligand, is only found in complex A. Furthermore, ILE304, present in the native ligand, is completely absent from complexes A, B, C, and D.

Table 4. Binding Interactions of the Co-crystallized Ligand with ALDH1A1 in the PDB 7UM9 Structure

Compound	Active Amino Acid	Bond Length	Bond Type	Bond Category
Native Ligand	CYS302	5,48636	Pi-Sulfur	Other
	CYS302	5,51284	Pi-Sulfur	Other
	TYR297	4,22045	Pi-Pi Stacked	Hydrophobic
	TYR297	3,87252	Pi-Pi Stacked	Hydrophobic
	TYR297	4,37716	Pi-Pi Stacked	Hydrophobic
	CYS303	5,3847	Alkyl	Hydrophobic
	ILE304	5,40549	Alkyl	Hydrophobic
	VAL460	4,91901	Alkyl	Hydrophobic
	PHE171	5,01138	Pi-Alkyl	Hydrophobic
	TRP178	5,17367	Pi-Alkyl	Hydrophobic

Specific interactions at key residues highlight the central role of TYR297, which is strongly involved in all complexes and the native ligand through Pi-Pi interactions with similar distances. Residue TRP178 establishes hydrogen and Pi-Alkyl bonds in complexes A, B, and D, with distances ranging from 2.0054 Å (complex D) to 2.2569 Å (complex A), while in the native ligand, this residue forms a hydrophobic interaction. Additionally, PHE171, involved in hydrophobic stability via Pi-Alkyl and Alkyl bonds, is observed in the native ligand (5.01 Å) as well as in complexes A, B, and C, where it interacts at a distance of 3.85 Å in complex A.

All the compounds studied interact significantly with the key residues PHE171, TYR297, and TRP178, which are involved in stabilizing the complex.

To better understand the interactions between compounds A, B, C, and D and ALDH1A1, an additional comparative analysis is presented below with reference to an experimental study.[28]

The key residues of ALDH1A1 involved in binding and inhibition by compounds such as CM026, CM053, and CM037[28] are identical to the residues discussed in our studies and can be cited: TYR297, TRP178, PHE171, VAL460, and CYS302.

These results suggest that complexes A, B, C, and D could represent promising candidates for future optimization, due to their high affinity and stability within the active site.

Compound A is the only molecule capable of forming a hydrogen bond with the GLY residue, a key component of the active site of the ALDH1A1 enzyme.[29] This interaction suggests that Compound A is the most promising candidate for further investigation.

ADMET Prediction

In drug development, many lead compounds are discarded after docking studies, emphasizing the critical role of meeting ADMET (Absorption, Distribution, Metabolism, Excretion, and Toxicity) criteria for successful drug development. These factors are essential in determining whether a compound can progress into a viable therapeutic agent.[30] The selected molecules were rigorously screened for ADMET properties, with the results as follows.

ADME Investigation and Drug-likeness

ADME evaluations provide an in-depth analysis of the physicochemical properties and drug-likeness predictions of the compounds.

Table 5. Physicochemical Properties of Theophylline Derivatives, Computed by ADMETlab

Parameters	Compound A	Compound B	Compound C	Compound D
MW	433.18	470.18	487.22	421.33
Rotatable Bonds	6	6	6	8
H-bond acceptors	9	9	9	10
H-bond donors	1	0	0	0
TPSA (E)	100.15	85.37	91.36	100.59
Consensus log P (Po/w)	2.85	2.86	3.30	2.80
Lipinski rules	Accepted	Accepted	Accepted	accepted

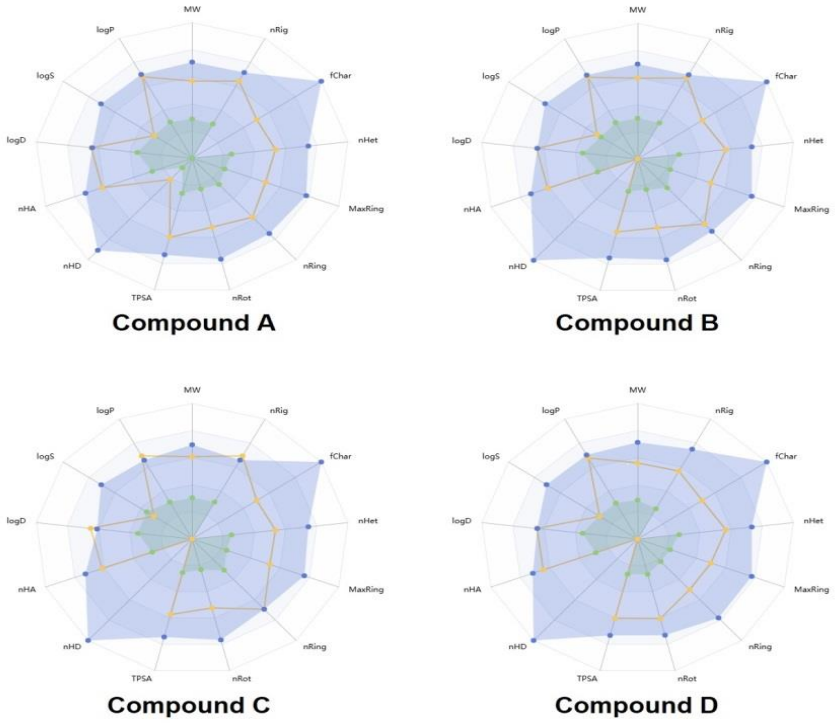

Figure 4. The Bioavailability Radar Plot (obtained from ADMETlab 3.0).

ADME Investigation and Drug-likeness

ADME evaluations provide an in-depth analysis of the physicochemical properties and drug-likeness predictions of the compounds.

Drug-likeness was assessed based on the Lipinski, Veber, and Ghose rules. According to Lipinski's filter[31] compounds with a molecular weight (MW) under 500 g/mol, a log *p* value < 5, and fewer than 5 hydrogen bond donors and 10 hydrogen bond acceptors are more likely to show favourable absorption. The Ghose rule[32] further refines drug-likeness, specifying a MW between 160 and 480, a log P between −0.4 and 5.6, and a molecular refractivity (MR) between 40 and 130. The Veber filter[33] additionally requires a polar surface area (PSA) ≤ 140 and no more than 10 rotatable bonds. All four compounds meet these established criteria (Table 5).

The bioavailability radar plot (Figure 5) generated by ADMETlab 3.0 confirms that all four compounds exhibit excellent drug-likeness. The compounds fall within the optimal ranges for drug absorption, permeability, and distribution, as indicated by the blue areas of the radar plot, while the yellow dots represent the specific properties of the molecules.

Pharmacokinetic Analysis

The pharmacokinetic analysis (Table 6) clearly differentiates the compounds in terms of their therapeutic potential. Compound B shows the highest solubility (–3.67), essential for oral bioavailability, while compound D has the highest clearance (3.28 ml/min/kg), indicating faster systemic elimination. All compounds display excellent intestinal absorption and minimal P-gp substrate interaction, favourable for oral administration and reducing efflux-based drug resistance. Notably, the compounds have poor central nervous system (CNS) penetration, minimizing the risk of CNS-related side effects. Enzyme inhibition profiles are critical for assessing potential drug-drug interactions. Compound C is a moderate inhibitor of CYP2C19 (++), while compound B and compound C

Table 6. Pharmacokinetics Parameters of Theophylline Derivatives, Computed by ADMETlab

Parameters	Compound A	Compound B	Compound C	Compound D
Solubility (LogS)	-4.02	-3.67	-4.72	-4.05
Volume of distribution (VDss)	-0.03	0.03	0.02	0.25
HIA	Excellent	Excellent	Excellent	Excellent
BBB access	-	+++	+	--
P-gp substrate	-	--	--	--
CYP2C19 inhibitor	-	+++	+++	--
CYP2C9 inhibitor	+++	+++	---	++
CYP3A4 inhibitor	---	+++	+	---
Caco-2 Permeability	-4.79	-5.21	-4.79	-4.81
CL (ml/min/kg)	1.52	1.04	0.89	3.28

Table 7. Toxicity Prediction of Molecules Candidates

Molecules	Compound A	Compound B	Compound C	Compound D
Hepatotoxicity	Inactive	Inactive	Inactive	Inactive
Immunotoxicity	Inactive	Inactive	Active	Inactive
Cytotoxicity	Inactive	Inactive	Inactive	Inactive
Carcinogenicity	Inactive	Inactive	Inactive	Inactive
Cardiotoxicity	Inactive	Inactive	Inactive	Inactive
LD50 (mg/kg)	660	1600	660	772
Class	4	4	4	4

exhibit strong inhibition of CYP2C9 (+++). Compound A is a moderate inhibitor of CYP3A4 (+++), which may increase the risk of interactions with other drugs metabolized by these enzymes. Caco-2 permeability, reflecting the compound's ability to cross the intestinal barrier, is highest for A and C, both showing favourable values (–4.79), while compound B exhibits the lowest permeability (–5.21). This suggests that compound B may have reduced intestinal absorption compared to the others.

Toxicological Assessments

Toxicological predictions using Protox 3.0 (Table 7) show that all compounds are inactive in terms of hepatotoxicity, cytotoxicity, carcinogenicity, and cardiotoxicity, indicating a relatively low risk for organ toxicity. However, compound C is identified as having immunotoxic activity, which distin guishes it from the other molecules. The LD50 values range from 660 mg/kg (A and C) to 1600 mg/kg (compound B), suggesting that the compounds, in general, exhibit low acute toxicity. All molecules are classified as Class 4, confirming their relatively safe toxicity profiles for further development.

These compounds exhibit favourable ADMET profiles, making them strong candidates for further development. Compound B stands out due to its superior solubility, while compound D demonstrates high clearance. Compound A and compound C show high intestinal permeability, and all compounds shows a low toxicity risk class 4. The presence of immunotoxicity in Compound C warrants further investigation, though the overall safety profile of these compounds supports their potential for therapeutic use. These findings provide a clear direction for the next steps in the optimization of these compounds.

Molecular Dynamics Results

The molecular dynamics (MD) simulations conducted over 100 ns provide a definitive understanding of the ALDH1A1 ligand interactions, with all analyses supporting the binding behaviour observed in docking and ADMET studies.

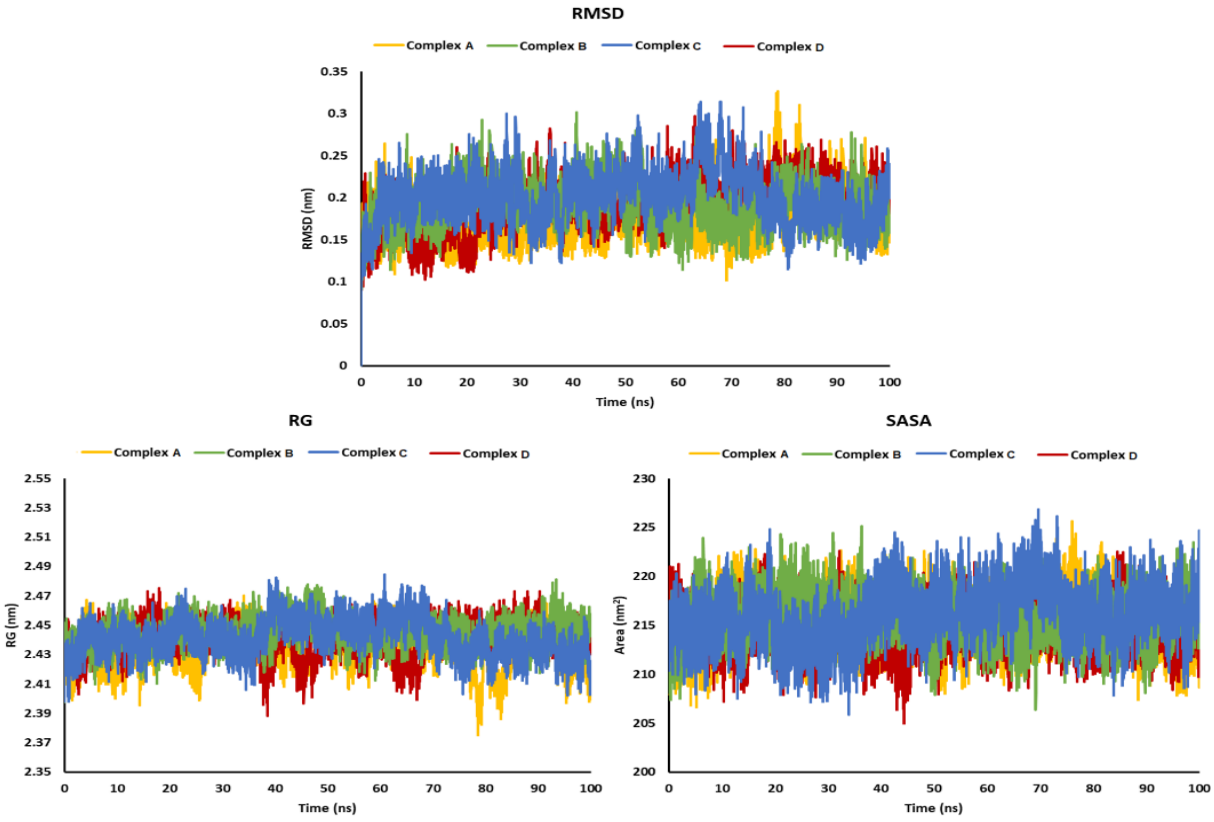

Figure 5. Global Structural Stability of the Complexes - RMSD, RG, and SASA over 100 ns MD Simulation.

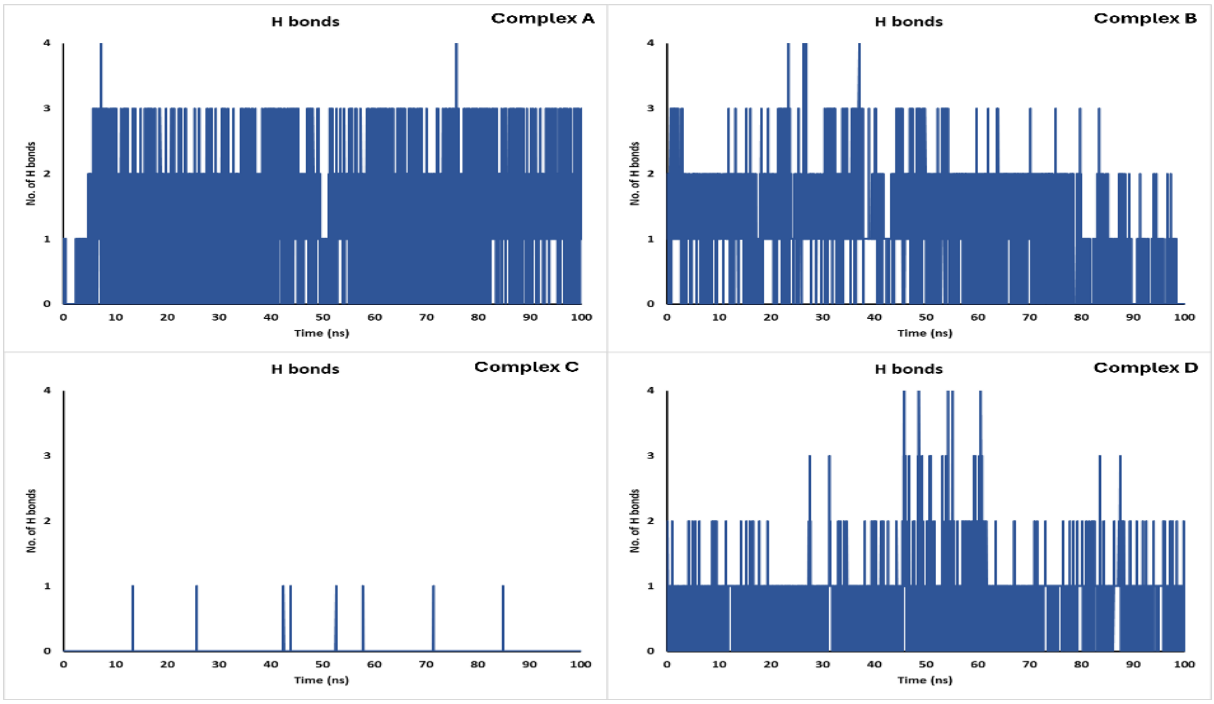

Figure 6. Total Hydrogen Bond Formation in Complexes A, B, C, and D during 100 ns MD Simulation.

Global Structural Stability

The root mean square deviation (RMSD), radius of gyration (RG), and solvent-accessible surface area (SASA) analyses demonstrate that the overall conformation of ALDH1A1 remains stable throughout the simulation (Figure 5), irrespective of the bound ligand. The consistent RMSD values (ranging from 0.17 ± 0.03 nm for compound A to 0.20 ± 0.03 nm for compound C) confirm that the protein's global structure is preserved. The constant RG (approximately 2.44 ± 0.01 nm) and stable SASA values (around 215 nm^2) establish that no significant conformational changes occur upon ligand binding, ensuring that variations in binding affinity stem from localized interactions rather than global protein rearrangements.

Local Interaction Dynamics and Hydrogen Bonding

The formation of hydrogen bonds is a definitive indicator of binding quality and specificity. Figure 6 shows in the compound A complex, the persistent formation of 2 to 3 hydrogen bonds during the entire simulation period confirms an optimal binding orientation within the ALDH1A1 active site. This stable network is responsible for the strong binding affinity measured by docking (-11.3 kcal/mol) and is further reinforced by direct interactions with important residues (TRP178, CYS 302, and TYR457).

For compound B and compound D, the dynamic hydrogen bond profiles exhibiting a consistent pattern of bond formation that ranges from 0 to 4 bonds demonstrate that although the binding is acceptable, the interaction is less rigid compared to compound A. The moderate variability in hydrogen bonding correlates with their respective ADMET profiles, where compound B benefits from superior solubility and compound D from a high clearance rate.

In contrast, the compound C complex shows an almost complete absence of sustained hydrogen bonds (Figure 6), which is directly attributed to steric hindrance and the lack of complementary functional groups. This deficiency is confirmed by significant fluctuations in local residue dynamics (particularly in the 466 - 475 loop region), and it accounts for the lower binding affinity and the less favourable ADMET profile, including immunotoxicity.

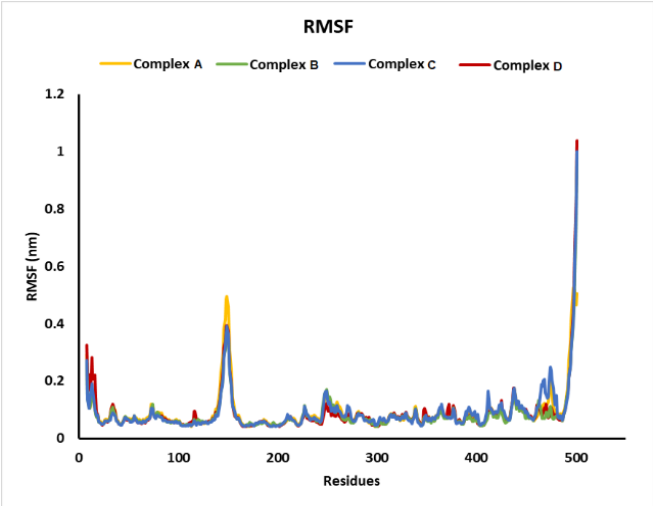

Figure 7. Root Mean Square Fluctuation (RMSF) of the Four Complexes over 100 ns of Molecular Dynamics Simulation.

Residue Flexibility and Local Dynamics

The root mean square fluctuation (RMSF) analysis confirms that local flexibility within the binding site plays a definitive role in ligand accommodation. In the compound A complex (Figure 7), controlled flexibility observed as a moderate increase in RMSF at residue 150 facilitates an induced fit mechanism that enhances the interaction.

In contrast, the excessive fluctuations seen in the compound C complex disrupt the proper alignment of binding residues, thereby impairing stable contact formation.

Conclusion

The combined results from docking, ADME, and toxicity assessments provide strong evidence for the potential of the four ALDH1A1 inhibitors as promising therapeutic candidates. Among them, compound A stood out as the strongest inhibitor, with an affinity of -11.3 kcal/mol. The compound demonstrated key interactions, including hydrogen bonds and hydrophobic forces, with important protein residues like TRP178, THR129, CYS302, and CYS303 which are important for stabilizing the ligand-protein complex. Moreover, compound A is noteworthy for its excellent pharmacokinetic properties due to its favourable absorption, lack of significant P-gp interaction, and lower risk of drug-drug interactions. MD simulations confirmed a stable global protein structure and revealed distinct local interaction patterns. Notably, compound A showed a robust hydrogen bond network, whereas compound C lacked these interactions. These findings align with the docking and ADMET results, guiding the rational optimization of ALDH1A1 inhibitors. However, some challenges remain, such as solubility, moderate toxicity, and possible P-gp interactions in some compounds. These factors point to the need for further refinement by formulation strategies and extensive safety studies. Despite these challenges, the compounds show promising pharma cokinetic profiles and strong binding affinities to suggest a good foundation for continued optimization. Overall, further in vitro and in vivo studies will be required to confirm their therapeutic efficacy and safety. Collectively, all these findings point to significant promise for these inhibitors in facilitating the development of novel treatments targeting pathologies related to ALDH1A1.

Authors' Contributions

FZF: Conceptualization, Investigation, Methodology, Data curation, Formal analysis, Writing original draft; NT: Supervision, Validation, Project administration; KS: Con ceptualization, Investigation, Methodology, Bibliographic research, Data curation, Formal analysis, Writing-review & editing; WC: Investigation, Bibliographic research, Data curation, Writing-review & editing; MAAT: Investigation, Data curation, Formal analysis, Writing-review & editing; SB: Investigation, Data curation, Formal analysis, Writing-review & editing; FS: Investigation, Formal analysis, Data curation; SM: Investigation, Formal analysis, Bibliographic research; KO: Investigation, Bibliographic research.

Conflict of Interest Disclosures

The authors declare that they have no conflicts of interest.

Acknowledgment

The authors sincerely acknowledge the General Direction of Scientific Research and Technological Development of Algeria (DGRSDT) and the Ministry of Higher Education and Scientific Research of Algeria (MESRS) for their financial support. Also, the authors acknowledge the Department of Physical Chemistry, Faculty of Pharmacy, University of Valencia, Spain.

References

1. Wei Y, Li Y, Chen Y, Liu P, Huang S, Zhang Y, et al. ALDH1: A potential therapeutic target for cancer stem cells in solid tumors. Front Oncol. 2022;12:1026278. doi:10.3389/fonc.2022.1026278
2. Liu C, Qiang J, Deng Q, Xia J, Deng L, Zhou L, et al. ALDH1A1 Activity in Tumor-Initiating Cells Remodels Myeloid-Derived Suppressor Cells to Promote Breast Cancer Progression. Cancer Res. 2021;81:5919–34. doi:10.1158/0008-5472.CAN-21-1337
3. Poturnajova M, Kozovska Z, Matuskova M. Aldehyde dehydrogenase 1A1 and 1A3 isoforms – mechanism of activation and regulation in cancer. Cell Signal. 2021;87:110120. doi:10.1016/j.cellsig.2021.110120
4. Clark DW, Palle K. Aldehyde dehydrogenases in cancer stem cells: potential as therapeutic targets. Ann Transl Med. 2016;4:518–518. doi:10.21037/atm.2016.11.82
5. Barnes PJ. Theophylline. Am J Respir Crit Care Med. 2013;188:901-6. doi:10.1164/rccm.201302-0388PP
6. Jung SM, Peyton L, Essa H, Choi DS. Adenosine receptors: Emerging non-opioids targets for pain medications. Neurobiology of Pain. 2022;11:100087. doi:10.1016/j.ynpai.2022.100087
7. Ruddarraju RR, Murugulla AC, Kotla R, Tirumalasetty MCB, Wudayagiri R, Donthabakthuni S, et al. Design, synthesis, anticancer activity and docking studies of theophylline containing 1,2,3-triazoles with variant amide derivatives. Medchemcomm. 2016;8:176. doi:10.1039/C6MD00479B
8. Ye J, Mao L, Xie L, Zhang R, Liu Y, Peng L, et al. Discovery of a Series of Theophylline Derivatives Containing 1,2,3-Triazole for Treatment of Non-Small Cell Lung Cancer. Front Pharmacol. 2021;12. doi:10.3389/fphar.2021.753676
9. Frisch MJ, Trucks GW, Schlegel HB, Scuseria GE, Robb MA, Cheeseman JR, et al. Gaussian 16, Revision C.01. Wallingford, CT: 2016.
10. Gasteiger J, Marsili M. A new model for calculating atomic charges in molecules. Tetrahedron Lett. 1978; 19:3181–4. doi:10.1016/S0040-4039(01)94977-9
11. Fadel FZ, Tchouar N, Belaidi S, Soualmia F, Oukil O, Ouadah K. Computational screening and QSAR study on a series theophylline derivatives as ALDH1A1 inhibitors. J Fundam Appl Sci. 2021;13:942-64. doi:10.4314/jfas.v13i2.17
12. Trott O, Olson AJ. AutoDock Vina: Improving the speed and accuracy of docking with a new scoring function, efficient optimization, and multithreading. J Comput

Chem. 2010;31:455-61. doi:10.1002/jcc.21334
13. Fuhrmann J, Rurainski A, Lenhof HP, Neumann D. A new Lamarckian genetic algorithm for flexible ligand-receptor docking. J Comput Chem. 2010;31:1911-8. doi:10.1002/jcc.21478
14. Baroroh SSi, M.Biotek. U, Muscifa ZS, Destiarani W, Rohmatullah FG, Yusuf M. Molecular interaction analysis and visualization of protein-ligand docking using Biovia Discovery Studio Visualizer. Indones J Comput Biol. 2023;2:22-30. doi:10.24198/ijcb.v2i1.46322
15. Yusuf D, Davis AM, Kleywegt GJ, Schmitt S. An alternative method for the evaluation of docking performance: RSR vs RMSD. J Chem Inf Model. 2008;48:1411-22. doi:10.1021/ci800084x
16. Lin J, Sahakian D, de Morais S, Xu J, Polzer R, Winter S. The Role of Absorption, Distribution, Metabolism, Excretion and Toxicity in Drug Discovery. Curr Top Med Chem. 2005;3:1125-54. doi:10.2174/1568026033452096
17. Fu L, Shi S, Yi J, Wang N, He Y, Wu Z, et al. ADMETlab 3.0: an updated comprehensive online ADMET prediction platform enhanced with broader coverage, improved performance, API functionality and decision support. Nucleic Acids Res. 2024;52:W422. doi:10.1093/nar/gkae236
18. Banerjee P, Kemmler E, Dunkel M, Preissner R. ProTox 3.0: a webserver for the prediction of toxicity of chemicals. Nucleic Acids Res. 2024;52:W513-20. doi:10.1093/nar/gkae303
19. Li Q, Cheng T, Wang Y, Bryant SH. PubChem as a public resource for drug discovery. Drug Discov Today. 2010;15:1052. doi:10.1016/j.drudis.2010.10.003
20. Kagami L, Wilter A, Diaz A, Vranken W. The ACPYPE web server for small-molecule MD topology generation. Bioinformatics. 2023;39. doi:10.1093/BIOINFORMATICS/BTAD350
21. Van Der Spoel D, Lindahl E, Hess B, Groenhof G, Mark AE, Berendsen HJC. GROMACS: fast, flexible, and free. J Comput Chem. 2005;26:1701-18. doi:10.1002/JCC.20291
22. Lindorff-Larsen K, Piana S, Palmo K, Maragakis P, Klepeis JL, Dror RO, et al. Improved side-chain torsion potentials for the Amber ff99SB protein force field. Proteins. 2010;78:1950-8. doi:10.1002/PROT.22711
23. Wu Y, Tepper HL, Voth GA. Flexible simple point-charge water model with improved liquid-state properties. J Chem Phys. 2006;124. doi:10.1063/1.2136877
24. Parrinello M, Rahman A. Polymorphic transitions in single crystals: A new molecular dynamics method. J Appl Phys. 1981;52:7182-90. doi:10.1063/1.328693
25. Abdul Amin Sk, Adhikari N, Gayen S, Jha T. Insight into the Structural Requirements of Theophylline-Based Aldehyde Dehydrogenase IAI (ALDHIAI) Inhibitors Through Multi-QSAR Modeling and Molecular Docking Approaches. Curr Drug Discov Technol. 2016;13:84-100. doi:10.2174/1570163813666160429115628
26. Narendra G, Raju B, Verma H, Sapra B, Silakari O. Multiple machine learning models combined with virtual screening and molecular docking to identify selective human ALDH1A1 inhibitors. J Mol Graph Model. 2021;107. doi:10.1016/j.jmgm.2021.107950
27. Tsou PS, Page NA, Lee SG, Fung SM, Keung WM, Fung HL. Differential Metabolism of Organic Nitrates by Aldehyde Dehydrogenase 1a1 and 2: Substrate Selectivity, Enzyme Inactivation, and Active Cysteine Sites. AAPS J. 2011;13:548. doi:10.1208/s12248-011-9295-4
28. Morgan C A, Hurley T D. Characterization of Two Distinct Structural Classes of Selective Aldehyde Dehydrogenase 1A1Inhibitors. J Med Chem. 2015;58:1964-75. doi:10.1021/jm501900s
29. Pequerula R, Veraa J, Giménez-Dejoza J, Crespoa I, Coinesb J, Portéa S, et al. Structural and kinetic features of aldehyde dehydrogenase 1A (ALDH1A) subfamily members, cancer stem cell markers active in retinoic acid biosynthesis. Archives of Biochemistry and Biophysics. Arch Biochem Biophys. 2020:108256. doi:10.1016/j.abb.2020.108256
30. Cheng F, Li W, Liu G, Tang Y. *In Silico* ADMET Prediction: Recent Advances, Current Challenges and Future Trends. Curr Top Med Chem. 2013;13:1273-89. doi:10.2174/15680266113139990033
31. Lipinski CA, Lombardo F, Dominy BW, Feeney PJ. Experimental and computational approaches to estimate solubility and permeability in drug discovery and development settings. Adv Drug Deliv Rev. 1997;23:3-25. doi:10.1016/S0169-409X(96)00423-1
32. Ghose AK, Viswanadhan VN, Wendoloski JJ. A knowledge-based approach in designing combinatorial or medicinal chemistry libraries for drug discovery. 1. A qualitative and quantitative characterization of known drug databases. J Comb Chem. 1999;1:55-68. doi:10.1021/cc9800071
33. Veber DF, Johnson SR, Cheng HY, Smith BR, Ward KW, Kopple KD. Molecular properties that influence the oral bioavailability of drug candidates. J Med Chem. 2002;45:2615-23. doi:10.1021/jm020017n